

ORIGINAL ARTICLE

Open Access



Eocene foraminiferal biofacies in Kutch Basin (India) in context of palaeoclimate and palaeoecology

Sonal Khanolkar^{1,2*} and Pratul Kumar Saraswati¹

Abstract

The Eocene Epoch passed through multiple hyperthermal events and recorded highest temperatures in the Cenozoic. Very few studies from Eocene palaeotropical sites have recorded changes in shallow marine foraminiferal assemblages. The present study investigates the foraminiferal biofacies of shallow marine successions from a palaeotropical site in western India (Kutch Basin) to understand the palaeoclimate and its impact on the ecology of foraminifera. The sections were biostratigraphically constrained using planktic and larger benthic foraminifera. Four biofacies are recognized by detrended correspondence analysis of the sample-wise distribution of foraminifera. Low diversity and dwarfed foraminifera characterize *Bulimina–Chiloguembelina* biofacies (SBZ5/6–SBZ10), corresponding to the interval of Paleocene–Eocene Thermal Maxima (PETM) and Eocene Thermal Maxima 2 (ETM 2). Rectilinear benthic foraminifera and biserial and triserial planktic foraminifera, typical of high runoff, upwelling or eutrophic conditions, are dominant taxa in this biofacies. The specialist taxa increased significantly in *Asterigerina–Cibicides* biofacies, corresponding to SBZ11 (Early Eocene Climatic Optimum, EECO), and the environment became oligotrophic. The *Jenkinsina–Brizalina* biofacies (E12) is distinguished by foraminiferal assemblage ecologically like that of *Bulimina–Chiloguembelina* biofacies. It is characterized by high abundance of rectilinear benthic foraminifera and bloom of triserial planktic foraminifera, suggesting eutrophy and high runoff at the initiation of Middle Eocene Climatic Optimum (MECO). The foraminifera were more diverse and abundant in *Cibicides–Nonion* biofacies. The highly diverse larger benthic foraminiferal assemblage in this biofacies, signify warm and clear-water oligotrophic sea that promoted the development of platform carbonate in Kutch Basin and other basins in western India. The EECO and MECO did not have an adverse impact on shallow marine foraminifera, and particularly the larger benthic foraminifera attained high diversity, high abundance, larger size and wider latitudinal distribution in the middle Eocene.

Keywords: Hyperthermal events, Shallow marine, Morphogroups, Carbonate platform, Stable isotopes, Eocene, Kutch Basin

1 Introduction

The palaeotropical, Eocene, shallow marine succession is well exposed in Kutch Basin of western India (Biswas 1992; Khanolkar and Saraswati 2015). It is a highly fossiliferous, mixed carbonate–siliciclastic succession comprising well-preserved foraminifera of early Eocene (shallow benthic zones: SBZ5/6 to SBZ11) and middle Eocene

(planktic zone: E11 to E13). Very few shallow marine palaeotropical sites in the world consist of both early Eocene and middle Eocene foraminiferal records which record changes in palaeoenvironment and palaeodepositional conditions (Hottinger 1998; Stassen et al. 2012; Boscolo Galazzo et al. 2013) in a globally warm climate.

The Cenozoic rocks of Kutch Basin have been explored for oil in the offshore field in the past decade, and numerous papers based on the exposed onland sections were published in reference to lithostratigraphy, biostratigraphy and sequence stratigraphy (Biswas 1992; Sarkar et al. 2012; Khanolkar and Saraswati 2015;

* Correspondence: sonal.k.12@gmail.com

¹Department of Earth Sciences, Indian Institute of Technology Bombay, Mumbai 400076, India

²Department of Earth Sciences, Indian Institute of Technology Kanpur, Kanpur 208016, India

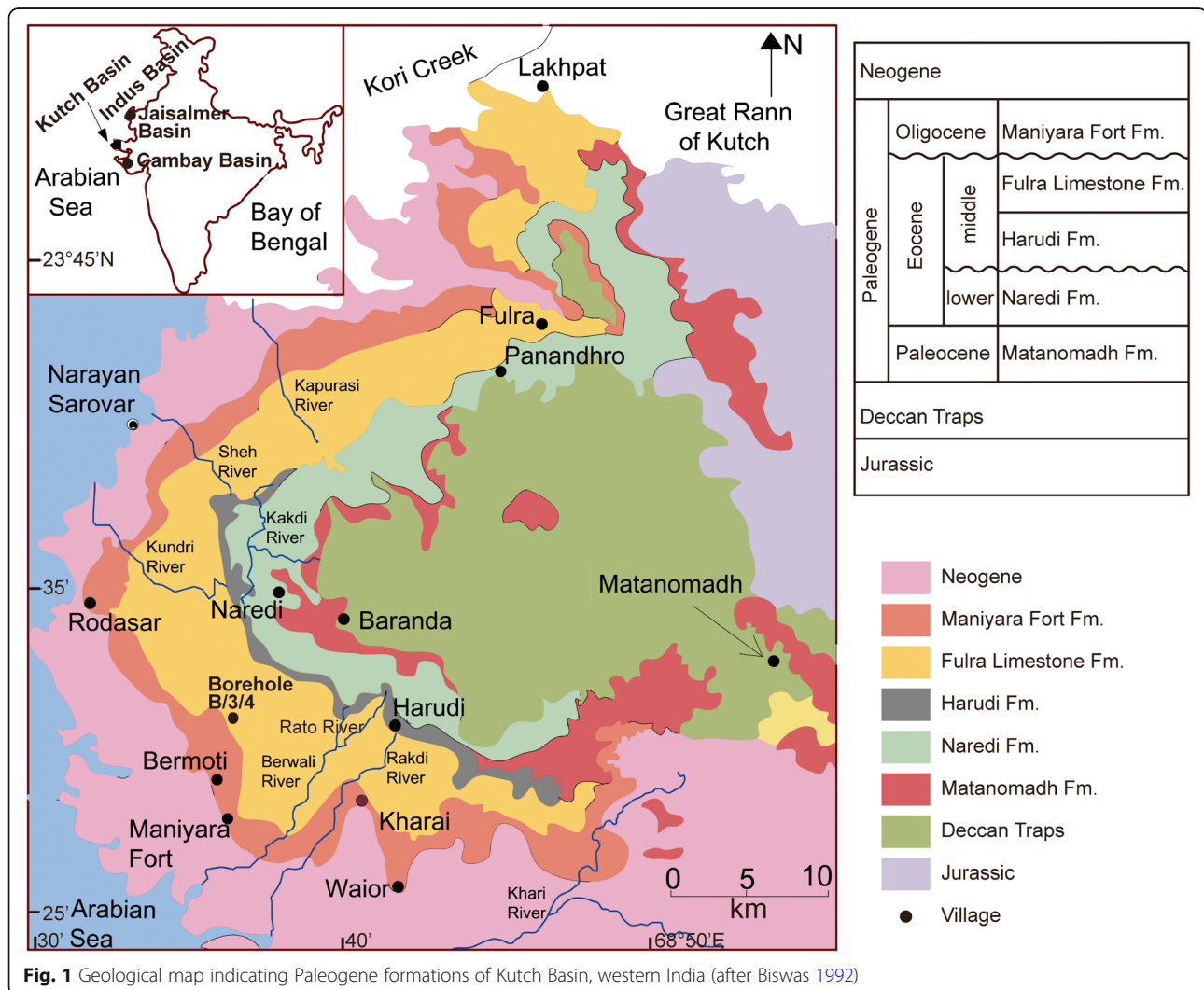
Saraswati et al. 2018). However, the distribution of foraminifera across the Eocene succession has not been detailed for statistical analysis to document the changes in foraminiferal biofacies. Further, the Eocene Epoch is punctuated by various hyperthermal events including the Paleocene–Eocene Thermal Maximum (PETM), Eocene Thermal Maximum 2 (ETM 2), Eocene Thermal Maximum 3 (ETM 3), Early Eocene Climatic Optimum (EECO) and Middle Eocene Climatic Optimum (MECO) (Zachos et al. 2001; Whidden and Jones 2012), and thus it would also be crucial to study this interval with respect to the changes in foraminiferal assemblages. The carbon isotope excursions (CIE) corresponding to the early and middle Eocene hyperthermal events have lately been established in Kutch Basin and the adjacent Cambay Basin (Clementz et al. 2011; Samanta et al. 2013; Saraswati et al. 2013; Khanolkar et al. 2017), and the oxygen isotopic data of foraminiferal carbonates of

Kutch Basin have been used to estimate the seawater temperatures of the Eocene time (Saraswati et al. 1993).

The main objectives of this study are to i) recognize the foraminiferal biofacies by statistical analysis of the foraminiferal data of the onland and borehole sections of Kutch Basin, and ii) record the palaeoecological changes in response to the multiple episodes of warming during the Eocene.

2 Geological setting

The Kutch Basin (Fig. 1) evolved in the Jurassic as a pericratonic rift basin and transformed in the Cenozoic to a passive-margin basin. It preserves a stratigraphic record of Jurassic to Holocene age with breaks in deposition at various intervals. The basin is delineated in the north by the Precambrian inliers of Nagar Parker, in the south by Saurashtra uplift and in the east by Radhanpur-Barmer Arch (Biswas 1987). On the west is the Arabian Sea where



a much thicker sequence of Cenozoic sediments is preserved on the present-day continental shelf than that exposed on land. The Cenozoic sedimentation is represented by about 900-m-thick sedimentary package, punctuated by several basin-wide unconformities and interpreted as several transgressive-regressive cycles. The Cenozoic succession is mainly developed in the western part of Kutch Basin and exposed along a narrow coastal plain trending approximately NW-SE. It is tectonically undisturbed and does not show signs of major folding or faulting. The beds are almost flat to low dipping at 1°–3° towards WSW. The Cenozoic sequence rests over Deccan Traps at some places and Mesozoic successions at the others.

The Eocene succession of Kutch Basin is classified into three lithostratigraphic units (Biswas 1992). The Cenozoic sediments overlie the Deccan Traps and at the base comprise of volcanoclastic sediments including trap-pebble conglomerate, pyroclastics and laterite. These terrestrial deposits constitute the Matanomadh Formation of probable Paleocene age. The lithostratigraphic units of the Eocene age are described below:

2.1 Naredi Formation

The stratotype of early Eocene Naredi Formation is exposed in Kakdi River section near the Naredi village. The Naredi Formation comprises shale and limestone

which is around 45 m in the borehole B/3/4 and approximately 18 m in the type section (Figs. 2a, 3a and b). It is subdivided into three members: i) the Gypsiferous Shale Member consisting of fossiliferous green glauconitic shales alternating with unfossiliferous red shales and intercalated gypsum layers (refer to Fig. 2a); ii) the *Assilina* Limestone Member consisting of bedded limestone and marls (Fig. 4a); and iii) the unfossiliferous Ferruginous Claystone Member found at the top of the section. The outcrops of the formation have yielded *Nummulites globulus nanus*, *N. burdigalensis kuepperi*, *N. burdigalensis cantabricus*, *N. burdigalensis burdigalensis*, *Assilina spinosa* and *A. laxispira*. A thicker section of the formation is recorded in a borehole that comprises *N. fraasi* and *N. solitarius* at the base. The sediments were deposited in a shallow marine environment with water depths ranging from 10 m to 30 m and highly fluctuating sea level in the lower part (Sarkar et al. 2012). The formation is overlain unconformably by Harudi Formation and the contact between the two formations is characterized by lateritic paleosol.

2.2 Harudi Formation

The total thickness of this formation is around 10 m. The lower part of the formation consists of carbonaceous shale and lignite lenses, and is devoid of any age

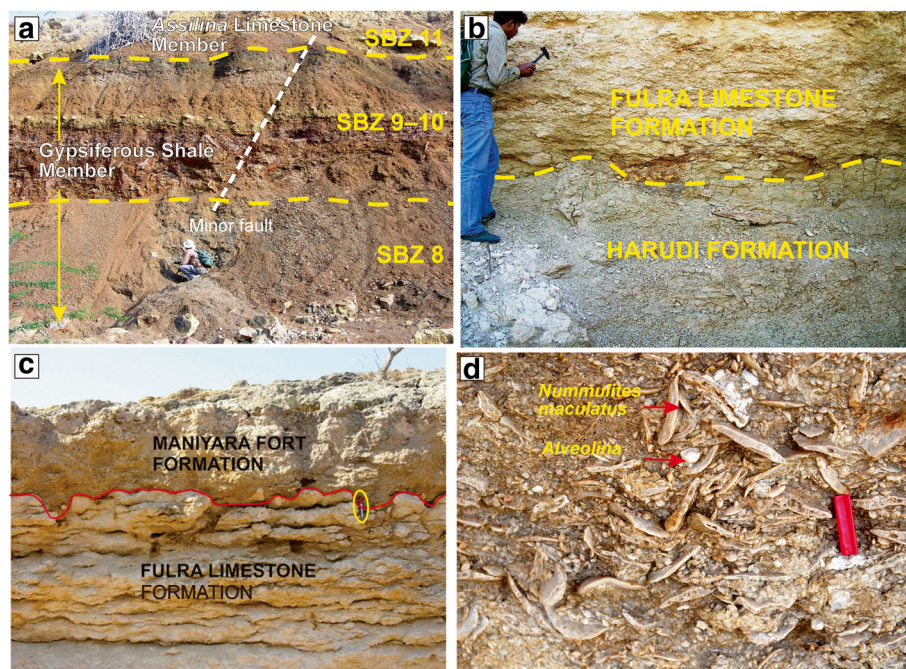
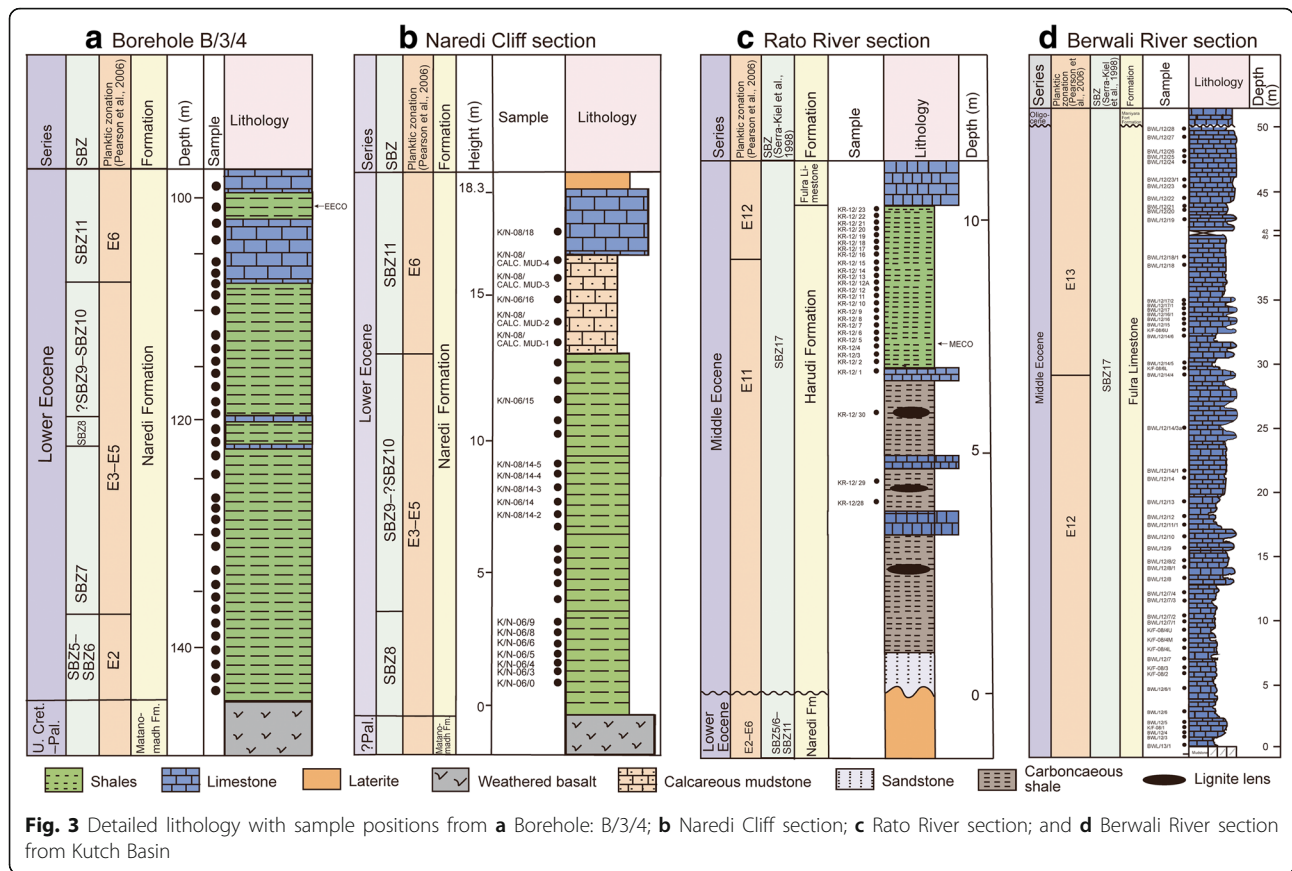


Fig. 2 Field photographs of Eocene formations in Kutch Basin. **a** Shales and limestone of Naredi Formation in the type locality exposed near Naredi village. Biostratigraphically the section extends from Zone SBZ8 to SBZ11 in Kakdi River section. Height of the person sitting is ~3 ft; **b** Contact between Harudi Formation and Fulra Limestone Formation, Rato River section. Height of the person is ~5.7 ft; **c** Palaeokarst surface (red line) between Fulra Limestone Formation and Maniyara Fort Formation. Length of the pen (circled) is 12 cm; **d** Close-up view of the upper part of Fulra Limestone Formation containing *Nummulites maculatus* and *Alveolina* sp. Length of the red rectangle object is 6 cm



diagnostic microfossil. The carbonaceous shale is interbedded with three coquina beds. The bioclasts found in these coquina beds consist of randomly oriented articulated bivalves and gastropods (Fig. 4b). The shales between the coquina beds contain a low abundance of smaller benthic foraminifera *Quinqueloculina* and *Cibicides*. The green shale occurs at the topmost part of the formation. The lower part of the green shale consists of larger benthic foraminifera namely *Nummulites obtusus*, *N. spectabilis* and *N. vredenburgi*. The green shale also exhibits planktic foraminifera (*Orbulinoides beckmanni*, *Acarinina rohri*, and *Streptochilus martini*) belonging to the Bartonian Age. Calcareous nannoplankton corroborates the Bartonian Age to this formation (Jafar and Rai 1994; Rai 1997). The grey shale and coquina beds were formed in shallow waters of ~5 m depths while the green shale was deposited at higher depths of ~15–60 m (Banerjee et al. 2012). A sharp change in lithology from shale-dominated Harudi Formation to Fulra Limestone Formation is observed (Fig. 2b).

2.3 Fulra Limestone Formation

It lies above the Harudi Formation and is distinguished by its light-colored limestone, dominantly consisting of larger benthic foraminifera (Fig. 2c, d). The middle

Eocene Fulra Limestone Formation as exposed along the Berwali River section is 50 m thick. The Fulra Limestone Formation sequence is a monotonous succession of carbonaceous mudstone, wackestone, packstone and grainstone varieties (Fig. 4c, d). It is a highly fossiliferous limestone mainly comprising of different types of larger benthic foraminifera including *Assilina exponents*, *Nummulites stamineus*, *N. beaumonti*, *N. discorbinus*, *N. vohrai*, *N. praediscorbinus*, *N. pinfoldi*, *N. maculatus*, *Discocyclusina augustae*, *Discocyclusina dispansa*, *D. sowerbyi*, *Discocyclusina kutchensis*, *Orbitoclypeus hynesii*, *Alveolina elliptica*, *Asterocyclusina alticostata* and *A. sireli* (Saraswati et al. 2000; Ben İsmail-Lattrache et al. 2013; Özcan et al. 2016). It can be inferred from foraminiferal assemblage that the Fulra Limestone Formation was deposited at water depths of 30–60 m (Chattoraj et al. 2012; Banerjee et al. 2018). The upper boundary of Fulra Limestone Formation with the Maniyara Fort Formation of Oligocene is an unconformity and marked by a regionally extensive palaeokarst surface (Fig. 2c). The Maniyara Fort Formation consists of shales and limestone (Saraswati et al. 2018).

3 Materials and methodology

The outcrops along rivers and a borehole section were selected for the present study. The positions of samples

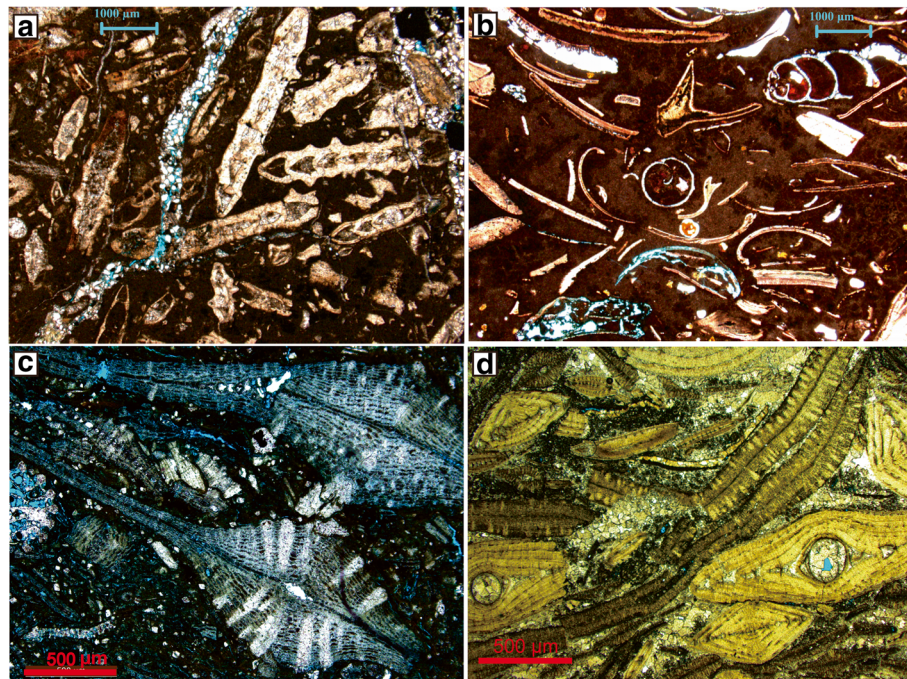


Fig. 4 Photomicrographs of **a** *Assilina* packstone, *Assilina* Limestone Member, Naredi Formation; **b** Molluscan packstone, Harudi Formation; **c** *Discocyclina* packstone, Fulra Limestone Formation; and **d** Nummulitic grainstone, Fulra Limestone Formation

in the lithologs of the traversed sections and the borehole are given in Fig. 3. For extraction of foraminifera, the samples were disaggregated by soaking in Na_2CO_3 solution and gently heating for 30 min. The residue was washed over 325 ASTM (44 μm) and 35 ASTM (500 μm) sieves. The washed residue was then dried at 60 °C temperature in an oven.

The foraminifera were identified using the works of Singh and Kalia (1970), Murray and Wright (1974), Kalia (1978), Pearson et al. (2006), and Loeblich and Tappan (2015). The identified species are listed in the Additional file 1: Table S1. For quantitative analysis, a representative split comprising of approximately 300 planktic–benthic specimens were obtained from the >44 μm fraction using a microsplitter. The relative abundance of the taxa was calculated (Fig. 5 and Additional file 2: Table S2). The total foraminiferal number per gram was then calculated and plotted. However, for statistical analysis we have used the foraminiferal percentage data. The most representative taxa were gold coated before their observation by scanning electron microscope (SEM; Fig. 6). The micrographs were taken using the SEM instrument FEI QUANTA-200. The Fisher (α), and Shannon-Weaver (H) indices (Fig. 7) were calculated and detrended correspondence analysis (DCA; Figs. 8 and 9) were carried out using the PAST package (Hammer et al. 2001). We have used the foraminiferal species >5% in any sample for statistical analysis. The data were subjected to detrended

correspondence analysis, so that (i) samples with similar taxonomic compositions and (ii) taxa with similar distributions across samples are placed close to each other. It is possible to place both samples and taxa on the same plot to visualize taxa–samples association. However, to avoid cluttering of data points we have plotted them separately (Figs. 8 and 9). The palaeoecological preferences of Eocene foraminifera found in Kutch is compiled in the Additional file 3: Table S3, which has been used for interpretations.

The morphogroups of foraminifera are widely used to interpret the palaeodepositional conditions (Nagy 1992; Preece et al. 1999; Nigam et al. 2007; Reolid et al. 2008; Singh et al. 2015). Two morphogroups of foraminifera are recognized: i) the rectilinear benthic foraminifera (RBF) and the rounded benthic foraminifera (RoBF). The RBF consist of genera with uniserial, biserial and triserial or uniserial chamber arrangements, and the RoBF include genera with trochospiral or planispiral chamber arrangements.

4 Biostratigraphy

4.1 Early Eocene

The stratigraphic positions of the early Eocene hyperthermal events are globally well constrained by biostratigraphy and magnetostratigraphy (Agnini et al. 2009; Whidden and Jones 2012). The planktic foraminifera are few and long ranging in Kutch Basin, and hence to provide a better estimate of age; the shallow benthic

zone (SBZ; Serra-Kiel et al. 1998) is used. According to the publications cited above, the PETM falls in SBZ5, ETM 2 in SBZ8, ETM 3 in the basal part of SBZ10 and EECO spans across the SBZ10–11. The SBZ5/6 in the borehole section B/3/4 is delineated by the presence of *Nummulites fraasi* and *N. solitarius*. The SBZ8 is delineated in the Naredi Cliff section and the borehole B/3/4 by the presence of *N. globulus nanus* and *N. burdigalensis kuepperi*. The SBZ11 is delineated in both the Naredi Cliff section and the borehole B/3/4 samples by the presence of *N. burdigalensis cantabricus* and *Assilina spinosa* (Saraswati et al. 2012; Saraswati et al. 2018).

4.2 Middle Eocene

In the middle Eocene, *Streptochilus martini*, *Acarinina rohri* and *Globoturborotalita ouachitaensis* define the zone E11, and the total range of occurrence of *Orbulinoides beckmanni* defines E12. The shale and lignite were deposited during E11, while the bulk of carbonates formed in the zones E12 and E13. The larger foraminiferal assemblage refers the formation to SBZ17 and is assigned to Bartonian age (Saraswati et al. 2018).

5 Results

The detrended correspondence analysis (DCA) assigned the studied samples into four groups with distinct correspondence scores (Fig. 8). The samples with similar taxonomic compositions are plotted close to each other and the respective groups represent distinct biofacies (I to IV). The R-mode (row mode) DCA plots the taxa with similar distributions across samples close to each other (Fig. 9). The clusters A to E (Fig. 9) are present in varying proportions in the four biofacies (Fig. 8). It is observed that each of the four biofacies (Fig. 8) is characterized by the most dominant occurrence of one of the clusters (Fig. 9) from A to D, while the species of cluster E occur uniformly in all biofacies, constituting on an average of 12% to 25% of the assemblage. Further, ecologically characteristic and consistently occurring taxa in samples corresponding to each biofacies are used in naming the biofacies. The characteristics of four biofacies, their ecological aspects and their biostratigraphic positions are discussed below.

5.1 *Bulimina–Chiloguembelina* biofacies (Biofacies I; Fig. 10a)

The biofacies is defined by high row scores on axis 1 and low row scores on axis 2. It is typically characterized by a high percentage (>55%) of the cluster A species (Fig. 9). *Bulimina* cf. *thantensis* is consistently abundant, forming >20% abundance in practically all the samples of this biofacies. The next abundant species is triserial planktic foraminifer *Chiloguembelina trinitatensis*. The associated taxa include infaunal foraminifera *Rotalia*, *Brizalina* and *Sagrina*. The samples belonging to this biofacies correspond to

shallow benthic zones SBZ5/6–SBZ8. The assemblage is found in glauconitic shales of the early Eocene Naredi Formation that is interpreted to have deposited in lagoonal to marginal marine conditions. The foraminifera in this assemblage are dwarf and are low to moderate in abundance.

5.2 *Asterigerina–Cibicides* biofacies (Biofacies II; Fig. 10b)

This biofacies is defined by moderate row scores on axis 1 and low row scores on axis 2. The species of cluster B (Fig. 9) in this biofacies is most abundant and constitute about 43% of the assemblage. The biofacies is characterized by a more diverse assemblage of both epifaunal and infaunal taxa as compared with that of the *Bulimina–Chiloguembelina* biofacies. *Asterigerina*, represented by two species, is most consistent and abundantly occurring genus in this biofacies and constitutes 50% of the populations in several samples. The associated taxa include a sizeable proportion of infaunal foraminifera *Nonion*, *Brizalina*, *Rotalia* and *Bulimina*. The triserial planktic foraminifera, *Chiloguembelina* and *Jenkinsina*, are virtually absent. This foraminiferal assemblage was found in the carbonates of lower Eocene Naredi Formation. The foraminiferal assemblage is indicative of open marine conditions and was deposited in SBZ11.

5.3 *Jenkinsina–Brizalina* biofacies (Biofacies III; Fig. 11a)

It is defined by low row scores on axis 1 and high row scores on axis 2. The species of cluster C is most abundant in this biofacies and constitutes about 52% of the assemblage (Fig. 9). *Jenkinsina columbiana*, a triserial planktic foraminifer, is most abundant and constitutes up to 65% of the foraminiferal population in some samples. *Brizalina* is the next common foraminifer in this biofacies that is associated with a few other infaunal taxa including *Trifarina*, *Nonion* and *Reussella*. This biofacies corresponds to planktic zones E11–E12 and shallow benthic zone SBZ17.

5.4 *Cibicides–Nonion* biofacies (Biofacies IV; Fig. 11b)

This biofacies is defined by low row scores on both the axes 1 and 2. The species of cluster D is most abundant (43%) in this biofacies (Fig. 9). The biofacies is distinguished by its most diverse assemblage of benthic foraminifera in the entire Eocene succession of Kutch Basin. *Cibicides* is represented by several species and it is the most abundant taxon in the assemblage. The other taxa include *Nonion*, *Nonionella*, *Florilus* and *Miliammina* that occur in varying proportions in the biofacies. The planktic foraminifer *Acarinina* is present in several samples, but triserial taxa including *Jenkinsina* are absent. This foraminiferal assemblage was found in the shales and carbonates of middle Eocene Harudi and Fulra Limestone Formations. The foraminiferal assemblage indicates

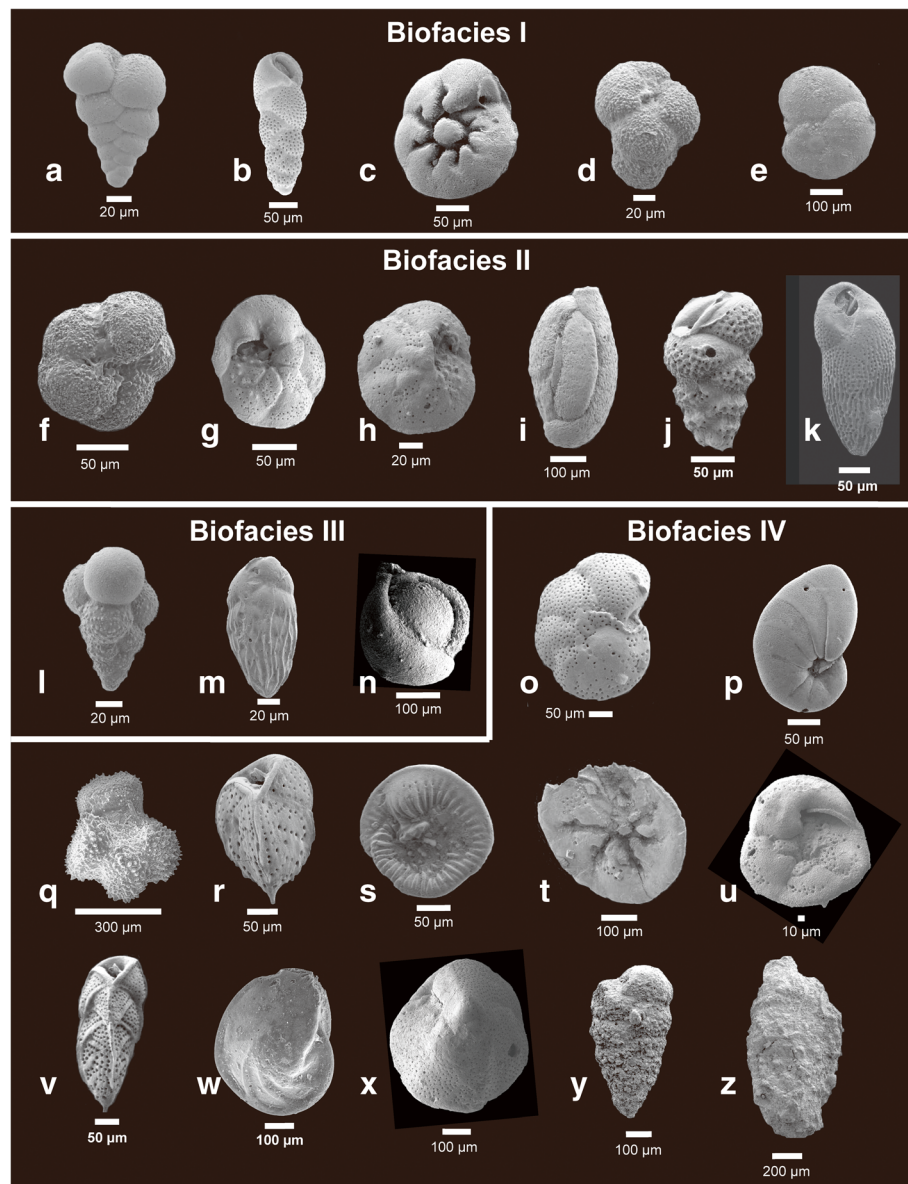


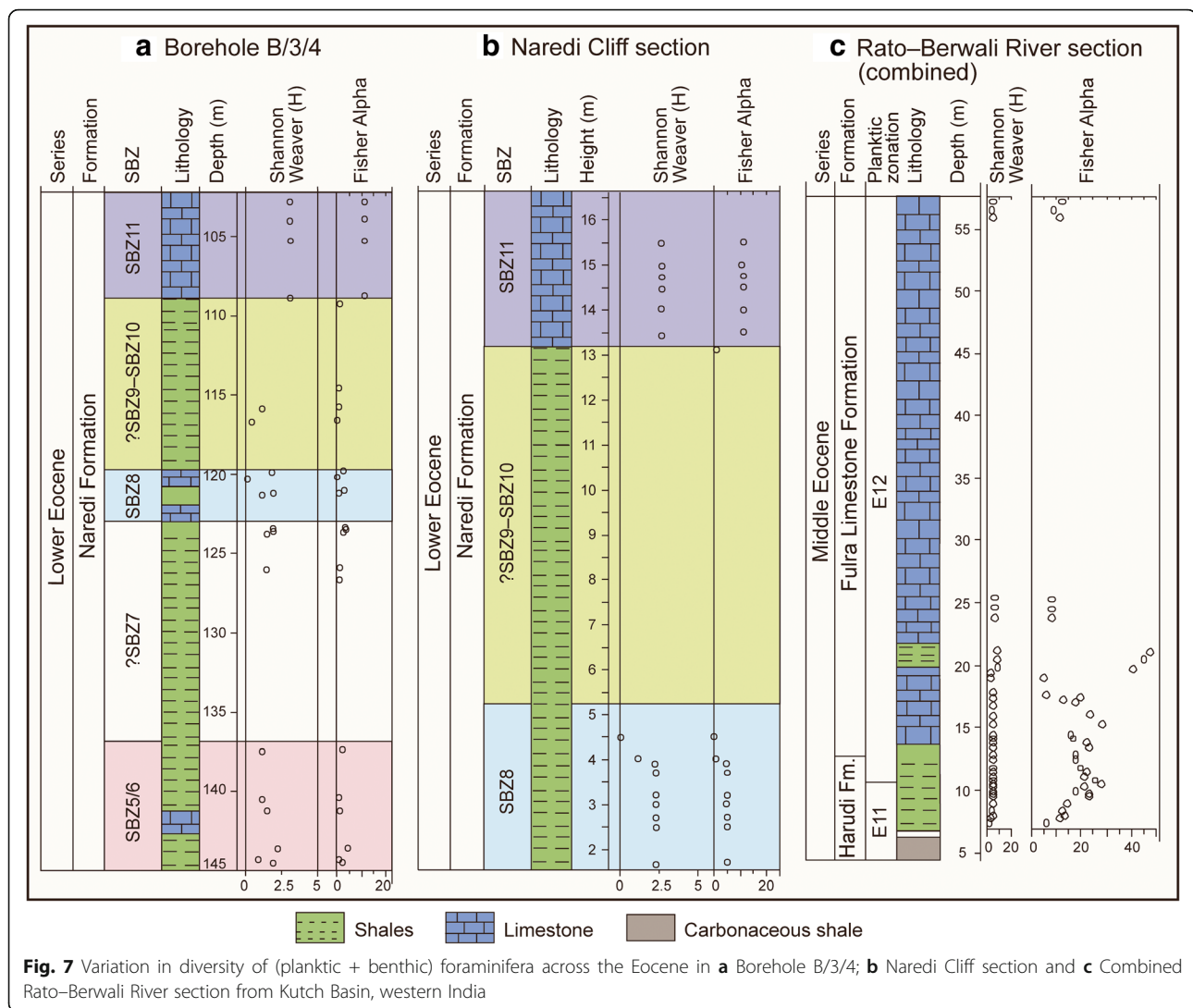
Fig. 6 The foraminiferal taxa in Eocene sections: **a–e** Biofacies I: **a** *Chiloguembelina trinitatensis*; **b** *Brizalina* cf. *oligocaenica*; **c** *Rotalia* sp.; **d** *Praebulimina* spp.; **e** *Rosalina* spp.; **f–k** Biofacies II: **f** *Pararotalia curryi*; **g** *Asterigerina*; **h** *Asterigerina bartoniana*; **i** *Quinqueloculina contorta*; **j** *Sagraia* sp.; **k** *Buliminella pupa*; **l–n** Biofacies III: **l** *Jenkinsina columbiana*; **m** *Brizalina* sp.; **n** *Triloculina architectura*; **o–z** Biofacies IV: **o** *Cibicides lobatulus*; **p** *Florilus* sp.; **q** *Acarinina topilensis*; **r** *Reussella* sp.; **s** *Glabratella ubiqa*; **t** *Neoeponoides schrebersii*; **u** *Pijpersia coronaeformis*; **v** *Trifarina advena rajasthanensis*; **w** *Robulus* sp.; **x** *Cibicides punjabensis*; **y** *Textularia halykardia*; **z** *Miliammina* cf. *fusca*

open marine environmental conditions and deeper water-depths compared with that of the Biofacies II. The samples of this biofacies correspond to the middle Eocene planktic zones E12–E13 and shallow benthic zone SBZ17.

6 Discussion

The Earth's climate was perturbed by multiple episodes of greenhouse and icehouse conditions during the Paleogene. It fluctuated from the extremes of warming

during the late Paleocene–early Eocene to glaciations during the late Eocene–early Oligocene (Kennett and Stott 1991; Miller et al. 1991; Zachos et al. 2001; Lourens et al. 2005; Nicolo et al. 2007; Stap et al. 2009). Some of these hyperthermal events have been delineated from Kutch Basin and adjacent Cambay Basin in western India (Clementz et al. 2011; Samanta et al. 2013; Saraswati et al. 2013; Khanolkar et al. 2017). It is interesting to study about the foraminiferal assemblages from

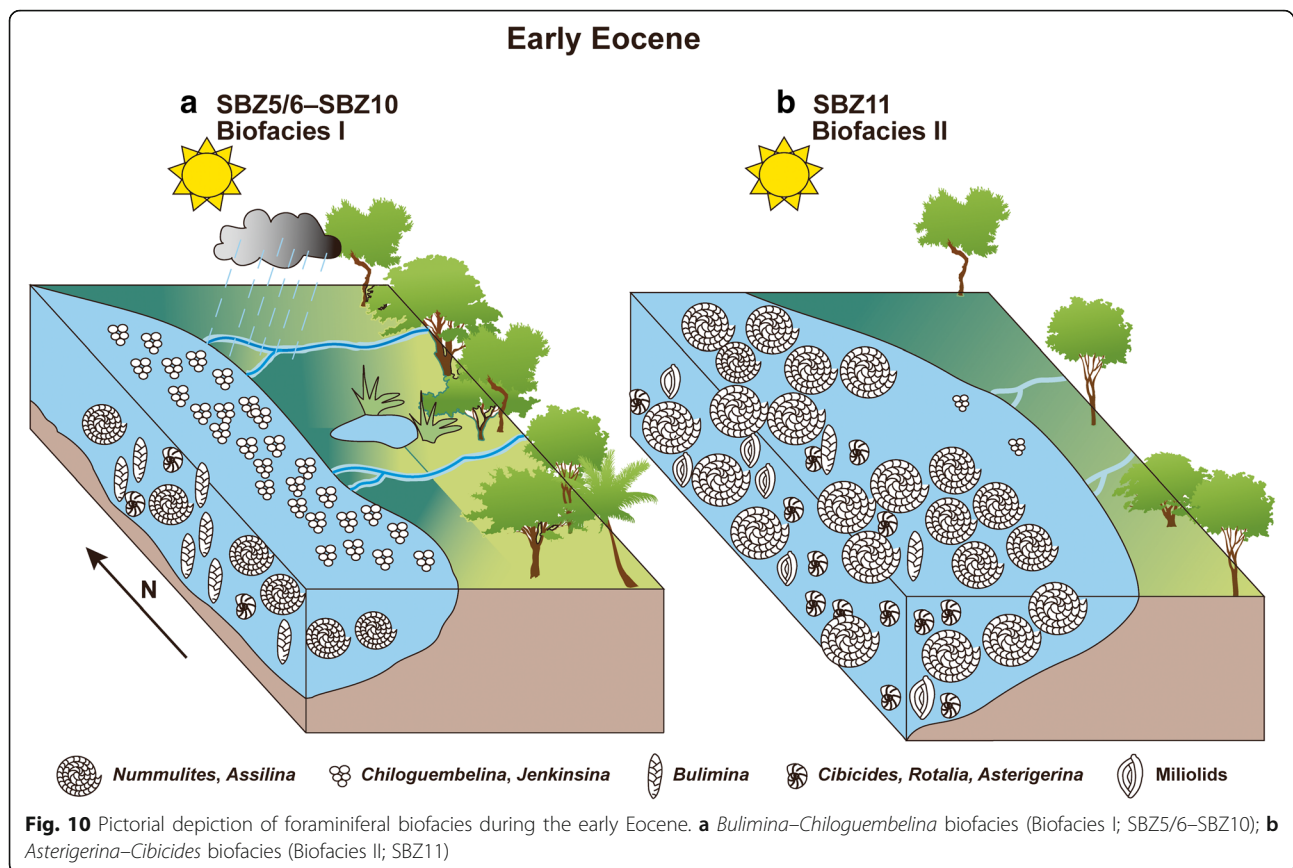


shallow marine palaeotropical sites such as Kutch Basin that how did they respond to the globally warm climate of the early and middle Eocene.

The Kutch Basin, on the western coast of India, has well-preserved and stratigraphically expanded sections of early and middle Eocene rocks containing shallow marine foraminifera (Khanolkar and Saraswati 2015; Khanolkar et al. 2017). The quantitative analysis of the foraminiferal data in the present study recognizes four biofacies across this succession. Each of the biofacies is characterized by typical assemblages of foraminifera signifying distinct ecological conditions. These are discussed below.

Chiloguembelina-*Bulimina* biofacies (Biofacies I; Fig. 10a) is referred to the SBZ5/6-SBZ10. The Biofacies I comprises of the shales belonging to the Naredi Formation which were deposited in four low-amplitude and low-frequency depositional cycles in an inner shelf environment (Saraswati et al. 2016). In the contemporaneous

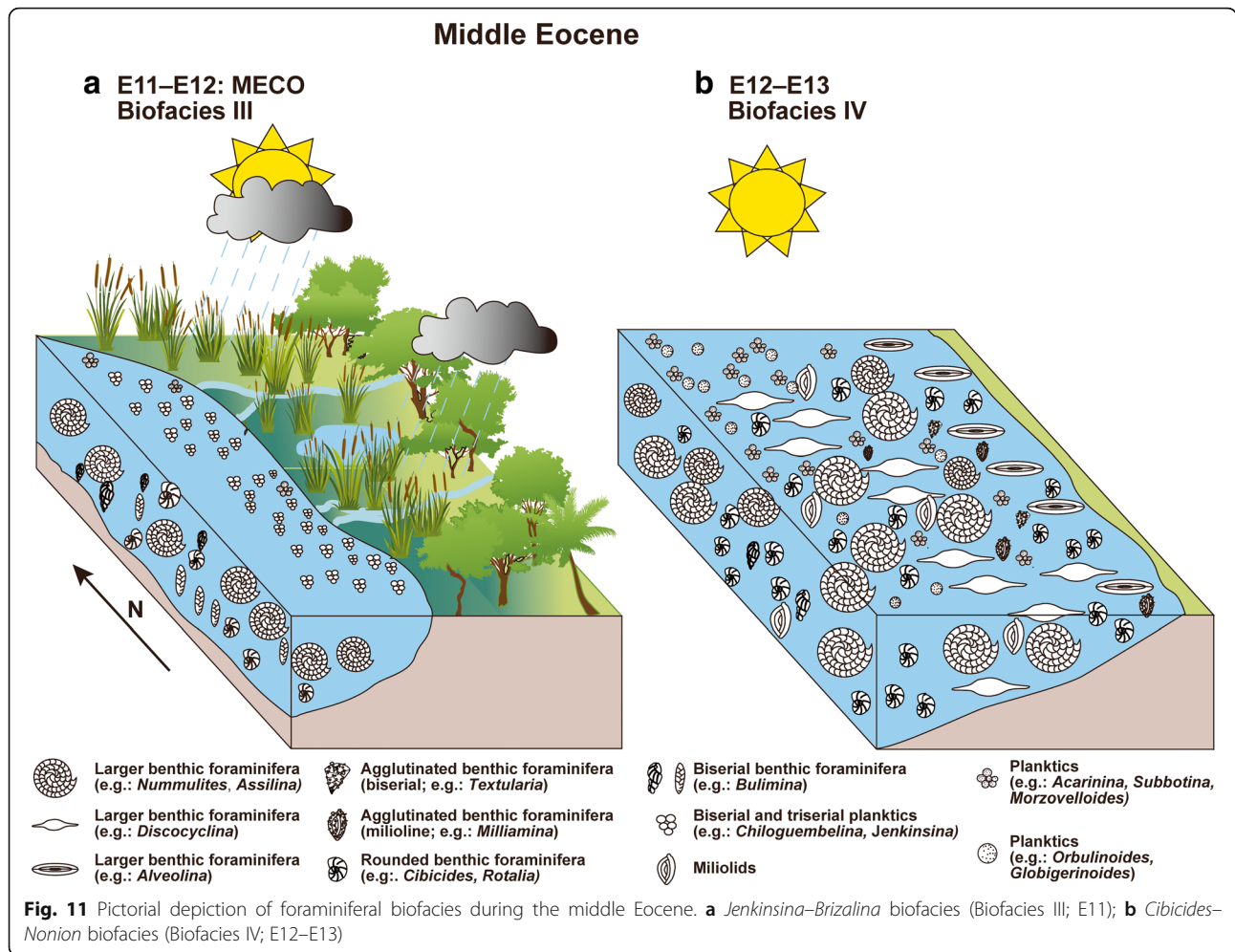
Cambay Basin (south of Kutch Basin; refer Fig. 1), two hyperthermal events, PETM and ETM 2, are recorded (Clementz et al. 2011; Samanta et al. 2013). The magnitude of negative CIE as recorded in the Cambay Basin is approximately ~5‰ for the PETM and 3‰-4‰ in the ETM 2. An extensive coal formation in the Cambay Basin during the PETM and ETM 2 (Sahni et al. 2006; Samanta et al. 2013) and the biomarkers of *Dipteocarpaceae* vegetation in the resins of lignite (Dutta et al. 2011) support a hot and humid climate with tropical rainforest in this region. The oxygen isotope data of *Nummulites* from these facies suggest temperatures of 32 °C (Saraswati et al. 1993). The *Chiloguembelina*-*Bulimina* biofacies (Biofacies I) records low Fisher Alpha and Shannon Weaver (H) diversity values as compared with *Asterigerina*-*Cibicides* biofacies (Biofacies II). Dwarfed biserial and triserial planktics (*Chiloguembelina* and *Jenkinsina*) and rectilinear benthic foraminifera (*Bulimina* and *Praebulimina*) dominate the foraminiferal assemblage. *C.*



and *Jenkinsina* indicate prevalence of high precipitation and surface runoff conditions which brought in the organic detritus from the landward side to the basin. The occurrence of *Rotalia* (~20%) and *Rosalina* (~10%) within this biofacies is indicative of marginal marine–hypersaline lagoon conditions (Khanolkar and Saraswati 2015). Dinoflagellates are also found in a low to moderate abundance within the shale-dominated Biofacies I compared with the above limestone-dominated Biofacies II (Garg et al. 2011). The dominance of algae (dinoflagellates), high percentage of biserial and triserial planktics, increase in surface runoff, and high precipitation probably led to increase in turbidity of the sea waters which created stressful conditions for the growth of algal-symbiont-bearing larger benthic foraminifera (LBF). The LBF, represented mainly by *Nummulites*, was low to moderate in abundance and confined to rare layers in this biofacies. The asexually reproduced, megaspherical generation (A-form) of *Nummulites* is dominant in this biofacies. Repetitive asexual reproduction might have caused dominant population of megaspherical generation (Dettmering et al. 1998) which is indicative of stressful environmental conditions like increase of nutritive supply in the basin, or a speedy increase of population in marginal environments

(Lipps 1982; Beavington-Penney and Racey 2004). The eutrophic condition during the PETM (SBZ5/6) also prevailed regionally as evidenced by the foraminifera of the Indus Basin. This makes the eastern Tethys (Kutch, Cambay, Rajasthan and Indus basins), markedly different from oligotrophy-dominated coeval shallow marine carbonates of the west Tethys (Scheibner and Speijer 2008). In the Kutch and Cambay basins, the eutrophic conditions prevailed upto the SBZ10.

The *Asterigerina–Cibicides* biofacies (Biofacies II; Fig. 10b), was deposited during the SBZ11, corresponding to the warming in EECO. The negative CIE of ~2‰ recorded from the Kutch Basin probably corresponds to EECO (Saraswati et al. 2014). There is a marked increase in diversity and abundance of foraminifera (Fisher Alpha: 10–11; Shannon Weaver H: 3.5) in comparison to Biofacies I. This Biofacies II, comprising of mudstones and grainstones was deposited at a water depth of about 30 m and constituted the maximum flooding surface within the early Eocene depositional sequence in the Kutch Basin (Saraswati et al. 2016). Miliolids and rounded benthic foraminifera including *Quinqueloculina*, *Spiroloculina*, *Cibicides*, *Asterigerina*, *Nonion* and *Florilus* became dominant in this biofacies indicating open marine conditions. The samples of this biofacies



correspond to SBZ11. The LBF consists of species of *Nummulites* and *Assilina* (Khanolkar and Saraswati 2015). The LBF increased in diversity, abundance and size signifying the change from eutrophic conditions of Biofacies I to oligotrophic in the Biofacies II (Fig. 12). The dinoflagellates, pollen and spores are scarce to absent in this biofacies (Garg et al. 2011). The drastic reduction and total absence of dinoflagellates, and biserial and triserial planktic foraminifera compared with Biofacies I indicate the prevalence of clear waters which promoted the growth of LBF (size of *Nummulites*, refer Fig. 12).



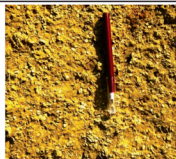
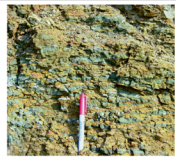
There is a substantial depositional gap (~7 myrs; Saraswati et al. 2018) between Naredi Formation (early Eocene: SBZ5/6–SBZ11) and Harudi Formation (late middle Eocene: E12) which has been recorded not just within the Kutch Basin but also in Indus Basin, Pakistan and Australian basins (McGowran et al. 2004; Saraswati et al. 2018) and is referred to as the Lutetian Gap. The sedimentation started after a major marine transgression during the late middle Eocene (E12) known to have flooded several basins in Australia, Pakistan and India, and is referred to as the

Kirthar/Wilson Buff transgression (Nagappa 1959; McGowran 1977, 1979; Raju 2008; Saraswati et al. 2018). This regional marine transgression was probably a result of the MECO warming event which has also been recorded in the Kutch Basin of India (Khanolkar et al. 2017). The negative CIE recorded in this biofacies is ~1.5‰ corresponding to MECO (Khanolkar et al. 2017). The *Jenkinsina–Brizalina* biofacies (Biofacies III; Fig. 11a) belonging to Harudi Formation (E11–E12) was deposited during the middle Eocene warming phase (Dutta 2007) and records the sudden increase in bathymetry as a response to this event (Khanolkar et al. 2017). The foraminiferal and palynomorph assemblages of the middle Eocene lignite deposits of Panandhro and Matanomadh mines within the Kutch Basin also indicate hot and humid conditions at the onset of the MECO (Saraswati et al. 2014; Khanolkar et al. 2017). The palynomorph analysis of the middle Eocene lignite mine sections of Kutch Basin further indicates angiosperm-dominated vegetation and an increase in diversity and abundance of dinoflagellates compared with the early Eocene lignite mine section of Cambay Basin (Sharma and Saraswati 2015;

Khanolkar and Sharma 2019). The Biofacies III, consisting of glauconitic shales was deposited at about 60 m water depth (the maximum flooding surface in the section) and constitutes a part of high-amplitude depositional cycle (Saraswati et al. 2016, 2018). The dominance of triserial and biserial planktics (*Jenkinsina* and *Chiloguembelina*) and high RBF% (25%–43%), in this biofacies are indicative of low oxygen, upwelling, high runoff and eutrophic conditions of deposition. Several new species such as *Nummulites obtusus*, *N. vredenburgi*, *N. spectabilis*, *Linderina* sp., and *Halkyardia* sp. appear in this biofacies. Megalospheric generation (A-forms) of *Nummulites* dominate the biofacies, nonetheless the microspheric generation (B-forms) are also common unlike the Biofacies I and II of early Eocene. There has been an increase in size and diversity of LBF in Biofacies III compared to Biofacies I and II, however, it remains less than in Biofacies IV. The high percentage of dinoflagellates, and organic input from land because of high runoff and upwelling conditions indicate eutrophic depositional conditions with increase in turbidity of water like Biofacies I. This probably has given rise to stressed conditions for the growth of LBF which otherwise flourish in clear and warm waters. The overall environment was like that of the Biofacies I (early Eocene) but it was somewhat less stressful for larger foraminifera as evidenced from a more diverse and larger size assemblages.

The oxygen isotope derived temperature was also significantly less at 26 °C for the seawater (Saraswati et al. 1993).

The most marked change in the Eocene succession occurred in the *Cibicides–Nonion* biofacies (Biofacies IV; Fig. 11b). This biofacies comprised of seven depositional cycles of high frequency out of which four were of low amplitude in inner shelf and three of high amplitude in middle shelf (Saraswati et al. 2016). The biofacies comprised mainly of mudstones, packstones and grainstones. The diversity and abundance of LBF community increased by several orders in comparison to the remaining biofacies of the area (refer to Fig. 7c). The common genera of LBF include *Nummulites*, *Assilina*, *Alveolina*, *Discocyclina*, *Dictyoconoides*, *Pellatispira* and *Asterocyclina*. The symbiont bearing LBFs are extremely sensitive to changes in light conditions (Hottinger 1983, 1998) and hence their depth distribution in the photic zone is dependent on the amount of nutrient flux (Hallock 1987, 1988). During the deposition of *Cibicides–Nonion* biofacies, the nutrient flux in the basin must have reduced giving rise to clear waters which facilitated the growth and diversity of LBF community. The size of the test of larger foraminiferal species and the number of microspheric generation (B-forms) in species of *Nummulites* increased, implying reduction in stressed conditions. This biofacies is dominated by larger

Thermal events	Biozone	Formation and lithology	Isotopic characteristics	Characteristics of foraminiferal assemblage				Field photographs of representative biofacies	
				Fisher Alpha	Size of <i>Nummulites</i>	RBF%	Biserial and triserial planktics (%)		Foraminiferal biofacies and palaeoenvironment
MECO	E12–E13	Fulra Limestone (carbonates) Harudi Formation (glauconitic shales)	$\delta^{13}C_{org}$: -25.8‰ to -24.2‰ ⁽⁵⁾	13–47	<i>N. vohrai</i> (A-form: 6–7.5 mm) (B-form: 8 cm) <i>N. maculatus</i> (A-form: 1.5–5 mm) (B-form: 16–37 mm)	7–24	1–10	<i>Cibicides–Nonion</i> biofacies (oligotrophic, open marine, large benthic dominant)	
	E11	Harudi Formation (carbonaceous and glauconitic shales)	Middle Eocene warming: $\delta^{13}C_{org}$: negative excursion of ~-1.5‰ ⁽⁵⁾ ; $\delta^{13}C_{carbonate}$: ~-3.5‰; $\delta^{18}O$: ~-0.5‰ ⁽⁶⁾	6–24	<i>N. obtusus</i> (A-form: 0.21–0.39 mm) (B-form: 7.4–26.2 mm)	25–43	27–70	<i>Jenkinsina–Brizalina</i> biofacies (eutrophic, low oxygen, high runoff, upwelling)	
EEOC	SBZ11	Naredi Formation (carbonates)	$\delta^{13}C_{org}$: negative excursion of ~-2‰ ⁽²⁾	10–11	<i>N. burdigalensis cantabricus</i> (A-form: ~1400 μm) (B-form: ~2300 μm)	10–20	10	<i>Asterigerina–Cibicides</i> biofacies (oligotrophic, open marine)	
ETM 3	SBZ10	Naredi Formation (glauconitic shales)	$\delta^{13}C_{org}$: negative excursion of ~-3‰–-4‰ ⁽³⁾	1–3	<i>N. burdigalensis burdigalensis</i> (A-form: ~1000 μm) (B-form: ~1700 μm)	50–70	<5	<i>Bulimina–Chiloguembelina</i> biofacies (eutrophic, low oxygen, high runoff)	
ETM 2	SBZ8		$\delta^{13}C_{org}$: negative excursion of ~-1‰ ⁽²⁾	3–5	<i>N. burdigalensis kuepperi</i> (A-form: ~1000 μm)	10–35	<5		
PETM	SBZ5/6		$\delta^{13}C_{org}$: negative excursion of ~-5‰ ⁽¹⁾	2–4	<i>N. solitarius</i> (A-form: ~600 μm)	10–40	60		

1. Samanta et al., 2013; 2. Saraswati et al., 2014; 3. Clementz et al., 2011; 4. Dutta 2007; 5. Khanolkar et al., 2017

Fig. 12 Summary of stable isotope characteristics and corresponding foraminiferal biofacies in the Kutch Basin, western India

benthic foraminifera and there is a significant reduction in the percentage of biserial/triserial planktics and RBF, indicating prevalence of oligotrophic conditions. The warm climate and the oligotrophic environment of the middle Eocene facilitated a regional growth of platform carbonates in Kutch Basin and the adjoining basins of Jaisalmer and Bombay offshore all of which are dominated by larger foraminifera.

7 Conclusions

The early to middle Eocene succession of Kutch Basin comprises of four foraminiferal biofacies, two of them correspond to early Eocene and the remaining two belong to the middle Eocene. The palaeoclimatic and palaeoecologic significance of the biofacies are as follows:

- 1) The *Bulimina–Chiloguembelina* biofacies (Biofacies I, SBZ5/6–SBZ10), corresponding to PETM and ETM 2, is characterized by low diversity assemblage of dwarfed foraminifera. The opportunistic triserial planktic foraminifera and rectilinear benthic foraminiferal morphogroup occurred in moderate to high abundance. This biofacies suggests eutrophic and dysoxic to suboxic environments.
- 2) The abundance and diversity of foraminifera increased significantly in *Asterigerina–Cibicides* biofacies (Biofacies II, SBZ11) of the EECO. The larger benthic foraminiferal genera increased in size, diversity and abundance. The transition from *Bulimina–Chiloguembelina* biofacies to *Asterigerina–Cibicides* biofacies was marked by a switch from eutrophic to oligotrophic environments and intermittently dysoxic to consistently suboxic conditions.
- 3) There is a bloom of triserial planktic and rectilinear benthic foraminifera in *Jenkinsina–Brizalina* biofacies (Biofacies III). It suggests eutrophy and high runoff associated with the initiation of the warming in middle Eocene (MECO). This biofacies is somewhat comparable to Biofacies I of the early Eocene but possibly less stressful for the larger foraminifera.
- 4) A marked increase in size, diversity and abundance of foraminifera is observed in *Cibicides–Nonion* biofacies (Biofacies IV). The warm and oligotrophic sea supported the growth of larger benthic foraminifera, the major source of carbonates in Kutch.

8 Additional files

Additional file 1: Table S1. List of foraminiferal species in this study. (DOC 109 kb)

Additional file 2: Table S2. Sample wise distribution of foraminifera data (percentage wise). (XLS 45 kb)

Additional file 3: Table S3. List of important foraminifera genera and their ecology. (DOC 46 kb)

Abbreviations

CIE: Carbon isotope excursions; DCA: Detrended correspondence analysis; EECO: Early Eocene Climatic Optimum; ETM: Eocene Thermal Maxima; LBF: Larger benthic foraminifera; MECO: Middle Eocene Climatic Optimum; PETM: Paleocene–Eocene Thermal Maxima; RBF: Rectilinear benthic foraminifera; RoBF: Rounded benthic foraminifera; SBZ: Shallow benthic zone; SEM: Scanning electron microscope

Acknowledgements

The authors like to thank IIT Bombay and IIT Kanpur for providing the research facilities. We are thankful to Prof. Robert Speijer for an initial review of this manuscript. SK would like to thank Department of Science and Technology (DST/INSPIRE/04/2016/002525) and University Grants Scheme for the funding provided to carry out this research work.

Funding

SK is thankful to University Grants Commission (UGC), India for providing the funds to carry out the research work.

Authors' contributions

SK carried out the foraminiferal analysis, participated in the field work and drafted the manuscript. PKS participated in the field work and drafted the manuscript. All authors have read and approved the final manuscript.

Competing interests

The authors declare that they have no competing interests. The authors alone are responsible for the content and writing of this article.

Publisher's Note

Springer Nature remains neutral with regard to jurisdictional claims in published maps and institutional affiliations.

Received: 17 August 2018 Accepted: 23 April 2019

Published online: 03 June 2019

References

- Agnini, C., P. Macrì, J. Backman, H. Brinkhuis, E. Fornaciari, L. Giusberti, V. Luciani, D. Rio, A. Sluijs, and F. Speranza. 2009. An early Eocene carbon cycle perturbation at ~52.5 Ma in the Southern Alps: Chronology and biotic response. *Paleoceanography* 24 (2): A2209.
- Banerjee, S., S.L. Chattoraj, P.K. Saraswati, S. Dasgupta, and U. Sarkar. 2012. Substrate control on formation and maturation of glauconites in the Middle Eocene Harudi Formation, western Kutch, India. *Marine and Petroleum Geology* 30 (1): 144–160.
- Banerjee, S., S. Khanolkar, and P.K. Saraswati. 2018. Facies and depositional settings of the Middle Eocene–Oligocene carbonates in Kutch. *Geodinamica Acta* 30 (1): 119–136.
- Beavington-Penney, S.J., and A. Racey. 2004. Ecology of extant nummulitids and other larger benthic foraminifera: Applications in palaeoenvironmental analysis. *Earth-Science Reviews* 67 (3–4): 219–265.
- Ben İsmail-Lattrache, K., E. Özcan, K. Boukhalfa, P.K. Saraswati, M. Soussi, and L. Jovane. 2013. Early Bartonian orthoherminids (Foraminiferida) from Reineche Limestone, North African platform, Tunisia: Taxonomy and paleobiogeographic implications. *Geodinamica Acta* 26 (1–2): 94–121.
- Biswas, S.K. 1987. Regional tectonic framework, structure and evolution of the western marginal basins of India. *Tectonophysics* 135 (4): 307–327.
- Biswas, S.K. 1992. Tertiary stratigraphy of Kutch. *Journal of the Palaeontological Society of India* 37: 1–29.
- Boscolo Galazzo, F., L. Giusberti, V. Luciani, and E. Thomas. 2013. Palaeoenvironmental changes during the Middle Eocene Climatic Optimum (MECO) and its aftermath: The benthic foraminiferal record from the Alano section (NE Italy). *Palaeogeography, Palaeoclimatology, Palaeoecology* 378: 22–35.
- Chattoraj, S.L., U. Sarkar, S. Chakraborty, S. Banerjee, and P.K. Saraswati. 2012. Facies and palaeogeography of the Middle Eocene Fulra limestone, Kutch. *Journal Indian Association Sedimentologists* 31: 1–9.
- Clementz, M., S. Bajpai, V. Ravikant, J.G.M. Thewissen, N. Saravanan, I.B. Singh, and V. Prasad. 2011. Early Eocene warming events and the

- timing of terrestrial faunal exchange between India and Asia. *Geology* 39 (1): 15–18.
- Dettmering, C., R. Röttger, J. Hohenegger, and R. Schmaljohann. 1998. The trimorphic life cycle in foraminifera: Observations from cultures allow new evaluation. *European Journal of Protistology* 34 (4): 363–368.
- Dutta, S., S.M. Tripathi, M. Mallick, R.P. Mathews, P.F. Greenwood, M.R. Rao, and R.E. Summons. 2011. Eocene out-of-India dispersal of Asian dipterocarps. *Review of Palaeobotany and Palynology* 166 (1): 63–68.
- Dutta, S.K. 2007. *Integrated Biostratigraphy and Chemostratigraphy of Eocene Sequence, Kutch* [Master's thesis]. Indian Institute of Technology, Bombay, India.
- Garg, R., V. Prasad, B. Thakur, I.B. Singh, and K. Ateequzaman. 2011. Dinoflagellate cysts from the Naredi Formation, southwestern Kutch, India: Implication on age and palaeoenvironment. *Journal of the Palaeontological Society of India* 56 (2): 201–218.
- Hallock, P. 1987. Fluctuations in the trophic resource continuum: A factor in global diversity cycles? *Paleoceanography* 2 (5): 457–471.
- Hallock, P. 1988. Interoceanic differences in foraminifera with symbiotic algae: A result of nutrient supplies? *Proceedings of the 6th International Coral Reef Symposium*, Australia 1988.
- Hammer, O., D.A.T. Harper, and P.D. Ryan. 2001. PAST: paleontological statistics software package for education and data analysis. *Palaeontologia Electronica* 4 (1): 1–9.
- Hottinger, L. 1983. Processes determining the distribution of larger foraminifera in space and time. *Utrecht Micropaleontological Bulletin* 30: 239–253.
- Hottinger, L. 1998. Shallow benthic foraminifera at the Paleocene–Eocene boundary. *Strata* 9 (9): 61–64.
- Jafar, S.A., and J. Rai. 1994. Late Middle Eocene (Bartonian) calcareous nannofossils and its bearing on coeval post-trappean transgressive event in Kutch Basin, western India. *Geophytology* 24: 23–42.
- Kalia, P. 1978. Buliminds from the Middle Eocene of Rajasthan, India. *Journal of the Palaeontological Society of India* 21 (22): 44–48.
- Kennett, J.P., and L.D. Stott. 1991. Abrupt deep-sea warming, palaeoceanographic changes and benthic extinctions at the end of the Palaeocene. *Nature* 353 (6341): 225–229.
- Khanolkar, S., and P.K. Saraswati. 2015. Ecological response of shallow marine foraminifera to early Eocene warming in equatorial India. *Journal of Foraminiferal Research* 45 (3): 293–304.
- Khanolkar, S., P.K. Saraswati, and K. Rogers. 2017. Ecology of foraminifera during the middle Eocene climatic optimum in Kutch, India. *Geodinamica Acta* 29 (2): 181–193.
- Khanolkar, S., and J. Sharma. 2019. Record of early to middle Eocene paleoenvironmental changes from lignite mines, western India. *Journal of Micropalaeontology* 38 (1): 1–24.
- Lipps, J.H. 1982. Biology/paleobiology of foraminifera. *Studies in Geology, Notes for a Short Course* 6: 1–21.
- Loeblich, A.R., and H. Tappan. 2015. *Foraminiferal Genera and Their Classification*. New York: Springer.
- Lourens, L.J., A. Sluijs, D. Kroon, J.C. Zachos, E. Thomas, U. Röhl, J. Bowles, and I. Raffi. 2005. Astronomical pacing of late Palaeocene to early Eocene global warming events. *Nature* 435 (7045): 1083–1087.
- McGowran, B. 1977. Maastrichtian to Eocene foraminiferal assemblages in the northern and eastern Indian Ocean region: Correlations and historical patterns, in: *Indian Ocean Geology and Biostratigraphy*, edited by: J.R. Heirtzler, H.M. Bolli, T.A. Davies, J.B. Saunders, and J.G. Sclater. *American Geophysical Union Special Publication*: 417–458.
- McGowran, B. 1979. The Tertiary of Australia: Foraminiferal overview. *Marine Micropaleontology* 4: 235–264.
- McGowran, B., G.R. Holdgate, Q. Li, and S.J. Gallagher. 2004. Cenozoic stratigraphic succession in southeastern Australia. *Australian Journal of Earth Sciences* 51 (4): 459–496.
- Miller, K.G., J.D. Wright, and R.G. Fairbanks. 1991. Unlocking the Ice House: Oligocene–Miocene oxygen isotopes, eustasy, and margin erosion. *Journal of Geophysical Research - Solid Earth* 96 (B4): 6829–6848.
- Murray, J.W., and C.A. Wright. 1974. Palaeogene Foraminifera and palaeoecology, Hampshire and Paris Basins and the English Channel. *Special Papers in Palaeontology* 14: 1–129.
- Nagappa, Y. 1959. Foraminiferal biostratigraphy of the Cretaceous–Eocene succession in the India–Pakistan–Burma region. *Micropaleontology* 5 (2): 145–177.
- Nagy, J. 1992. Environmental significance of foraminiferal morphogroups in Jurassic North sea deltas. *Palaeogeography, Palaeoclimatology, Palaeoecology* 95 (1–2): 111–134.
- Nicolo, M.J., G.R. Dickens, C.J. Hollis, and J.C. Zachos. 2007. Multiple early Eocene hyperthermals: Their sedimentary expression on the New Zealand continental margin and in the deep sea. *Geology* 35 (8): 699–702.
- Nigam, R., A. Mazumder, P.J. Henriques, and R. Saraswati. 2007. Benthic foraminifera as proxy for oxygen-depleted conditions off the central west coast of India. *Journal of the Geological Society of India* 70 (6): 1047–1054.
- Özcan, E., P.K. Saraswati, M. Hanif, and N. Ali. 2016. Orthophragminids with new axial thickening structures from the Bartonian of the Indian Subcontinent. *Geologica Acta* 14 (3): 261–282.
- Pearson, P.N., R.K. Olsson, C. Hemblen, B.T. Huber, and W.A. Berggren (Eds.). 2006. *Atlas of Eocene Planktonic Foraminifera*. Fredericksburg, USA: Cushman Special Publication, 513 pp.
- Preece, R.C., M.A. Kaminski, and T.W. Dignes. 1999. Miocene benthonic foraminiferal morphogroups in an oxygen minimum zone, offshore Cabinda. *Geological Society, London, Special Publications* 153: 267–282.
- Rai, J. 1997. Scanning-electron microscopic studies of the late middle Eocene (Bartonian) calcareous nannofossils from the Kutch Basin, western India. *Journal of the Palaeontological Society of India* 42: 147–167.
- Raju, D.S.N. 2008. Phanerozoic cycles of sea level change on Indian Plate: An overview with a base chart. Paper presented at the meeting of GEO India Convention and Exhibition, Delhi, India.
- Reolid, M., F.J. Rodríguez-Tovar, J. Nagy, and F. Olóriz. 2008. Benthic foraminiferal morphogroups of mid to outer shelf environments of the Late Jurassic (Prebetic Zone, southern Spain): Characterization of biofacies and environmental significance. *Palaeogeography, Palaeoclimatology, Palaeoecology* 261 (3–4): 280–299.
- Sahni, A., P.K. Saraswati, R.S. Rana, K. Kumar, H. Singh, H. Alimohammadian, N. Sahni, K.D. Rose, L. Singh, and T. Smith. 2006. Temporal constraints and depositional palaeoenvironments of the Vastan lignite sequence, Gujarat: Analogy for the Cambay Shale hydrocarbon source rock. *Indian Journal of Petroleum Geology* 15 (1): 1–20.
- Samanta, A., M.K. Bera, R. Ghosh, S. Bera, T. Filley, K. Pande, S.S. Rathore, J. Rai, and A. Sarkar. 2013. Do the large carbon isotopic excursions in terrestrial organic matter across Paleocene–Eocene boundary in India indicate intensification of tropical precipitation? *Palaeogeography, Palaeoclimatology, Palaeoecology* 387: 91–103.
- Saraswati, P.K., S. Banerjee, U. Sarkar, S. Chakraborty, and S. Khanolkar. 2016. Eocene depositional sequences and cycles in Kutch. *Journal of Geological Society of India (Special Publication)* 6: 46–56. <https://doi.org/10.17491/cgsi/2016/105409>.
- Saraswati, P.K., S. Khanolkar, and S. Banerjee. 2018. Paleogene stratigraphy of Kutch, India: An update about progress in foraminiferal biostratigraphy. *Geodinamica Acta* 30 (1): 100–118.
- Saraswati, P.K., S. Khanolkar, D.S.N. Raju, S. Dutta, and S. Banerjee. 2014. Foraminiferal biostratigraphy of lignite mines of Kutch, India: Age of lignite and fossil vertebrates. *Journal of Palaeogeography* 3 (1): 90–98.
- Saraswati, P.K., P.K. Patra, and R.K. Banerji. 2000. Biometric study of some Eocene *Nummulites* and *Assilina* from Kutch and Jaisalmer. *Journal of the Palaeontological Society of India* 45: 91–122.
- Saraswati, P.K., R. Ramesh, and S.V. Navada. 1993. Palaeogene isotopic temperatures of western India. *Lethaia* 26 (1): 89–98.
- Saraswati, P.K., U. Sarkar, and S. Banerjee. 2012. *Nummulites solitarius* — *Nummulites burdigalensis* lineage in Kutch with remarks on the age of Naredi Formation. *Journal of the Geological Society of India* 79 (5): 476–482.
- Saraswati, P.K., R.H. Williams, A. Chattopadhyay, S. Khanolkar, R.E. Summons, and S. Dutta. 2013. Integrated biostratigraphy, carbon isotope stratigraphy and biomarker study of an early Eocene section in western India: Hyperthermal events and palaeoenvironment. 26th International

- Meeting on Organic Geochemistry, held in Costa Adeje, Tenerife, Spain, 15th–20th September.
- Sarkar, U., S. Banerjee, and P.K. Saraswati. 2012. Integrated borehole and outcrop study for documentation of sea level cycles within the Early Eocene Naredi Formation, western Kutch, India. *Journal of Palaeogeography* 1 (2): 126–137.
- Scheibner, C., and R.P. Speijer. 2008. Late Paleocene–early Eocene Tethyan carbonate platform evolution — A response to long- and short-term paleoclimatic change. *Earth-Science Reviews* 90 (3–4): 71–102.
- Serra-Kiel, J., L. Hottinger, E. Caus, K. Drobne, C. Ferrandez, A.K. Jauhri, G. Less, R. Pavlovec, J. Pignatti, and J.M. Samsó. 1998. Larger foraminiferal biostratigraphy of the Tethyan Paleocene and Eocene. *Bulletin de la Société géologique de France* 169 (2): 281–299.
- Sharma, J., and P.K. Saraswati. 2015. Lignites of Kutch, western India: Dinoflagellate biostratigraphy and palaeoclimate. *Revue de micropaléontologie* 58 (2): 107–119.
- Singh, A.D., A.K. Rai, K. Verma, S. Das, and S.K. Bharti. 2015. Benthic foraminiferal diversity response to the climate induced changes in the eastern Arabian Sea oxygen minimum zone during the last 30 ka BP. *Quaternary International* 374: 118–125.
- Singh, S.N., and P. Kalia. 1970. A new planktonic foraminifer from the middle Eocene of India. *Micropaleontology* 16 (1): 76–82.
- Stap, L., A. Sluijs, E. Thomas, and L. Lourens. 2009. Patterns and magnitude of deep sea carbonate dissolution during Eocene Thermal Maximum 2 and H2, Walvis Ridge, southeastern Atlantic Ocean. *Paleoceanography and Paleoclimatology* 24 (1). <https://doi.org/10.1029/2008PA001655>.
- Stassen, P., E. Steurbaut, A. Morsi, P. Schulte, and R. Speijer. 2012. Biotic impact of Eocene Thermal Maximum 2 in a shelf setting (Dababiya, Egypt). *Austrian Journal of Earth Sciences* 105 (1): 154–160.
- Whidden, K.J., and R.W. Jones. 2012. Correlation of Early Paleogene global diversity patterns of large benthic foraminifera with Paleocene and Eocene climatic events. *Palaios* 27 (4): 235–251.
- Zachos, J., M. Pagani, L. Sloan, E. Thomas, and K. Billups. 2001. Trends, rhythms, and aberrations in global climate 65 Ma to present. *Science* 292 (5517): 686–693.

Submit your manuscript to a SpringerOpen[®] journal and benefit from:

- Convenient online submission
- Rigorous peer review
- Open access: articles freely available online
- High visibility within the field
- Retaining the copyright to your article

Submit your next manuscript at ► [springeropen.com](https://www.springeropen.com)
